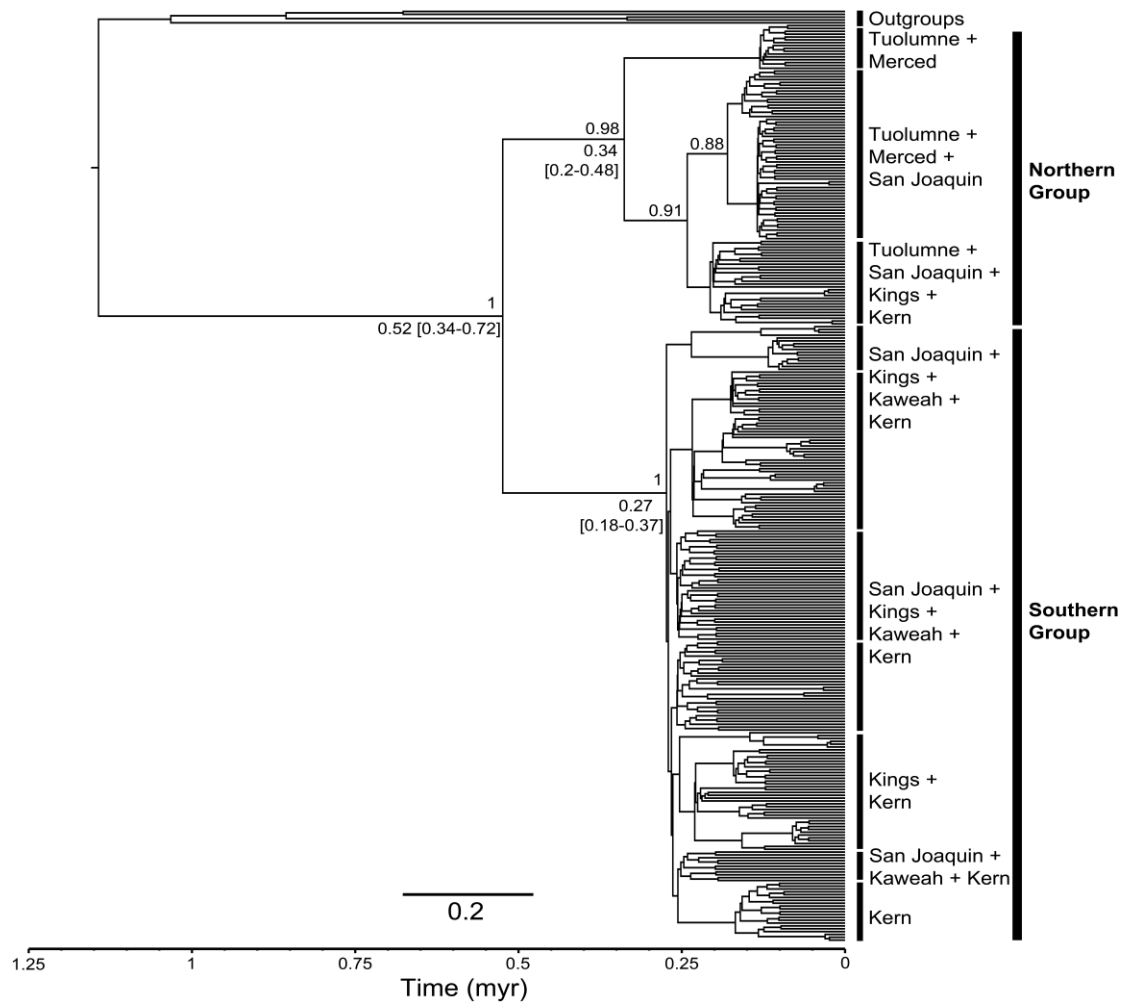


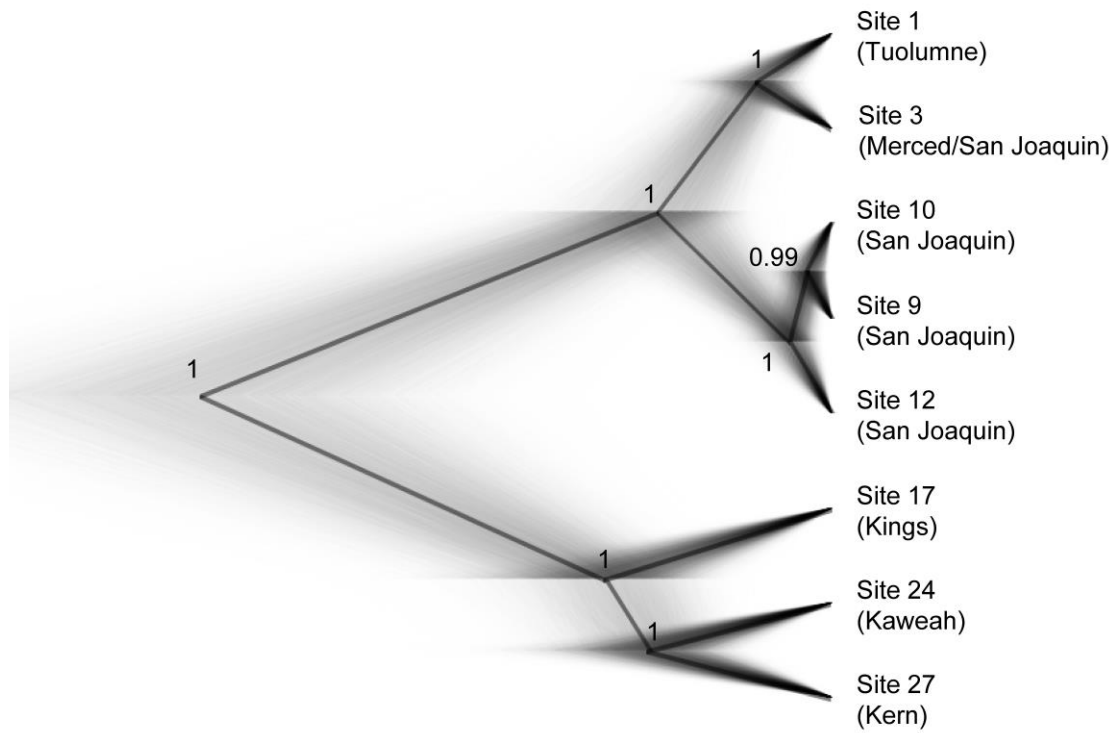
1
 2 **Figure 1.** Sample sites of the *Nebria ingens* complex in the Sierra Nevada, California.
 3 Collecting sites of *N. riversi*, the intermediate morphotype, and *N. ingens* are depicted
 4 with solid triangles, squares, and circles, respectively. The survey sites where no
 5 populations were located (despite survey efforts) are denoted by x marks. The extent
 6 of last glacial maximum is shown as a grey line (Rood, Burbank, & Finkel, 2011).
 7 Geographical names for each site can be found in **Table 2**

8
 9
 10



11
12
13
14
15
16
17
18
19
20

Figure 2. The Bayesian mitochondrial COI gene tree of the *Nebria ingens* complex with posterior probabilities listed above the nodes and divergence time listed beneath the nodes. Divergence time is estimated using a strict molecular clock (0.0113 substitutions per lineage per million years) and is denoted by the mean and 95% confidence interval. The two major clades correspond to a northern clade consisting of *N. riversi*, intermediate morphotypes, and some *N. ingens* samples, and a southern clade consisting solely of the intermediate morphotype and *N. ingens*.

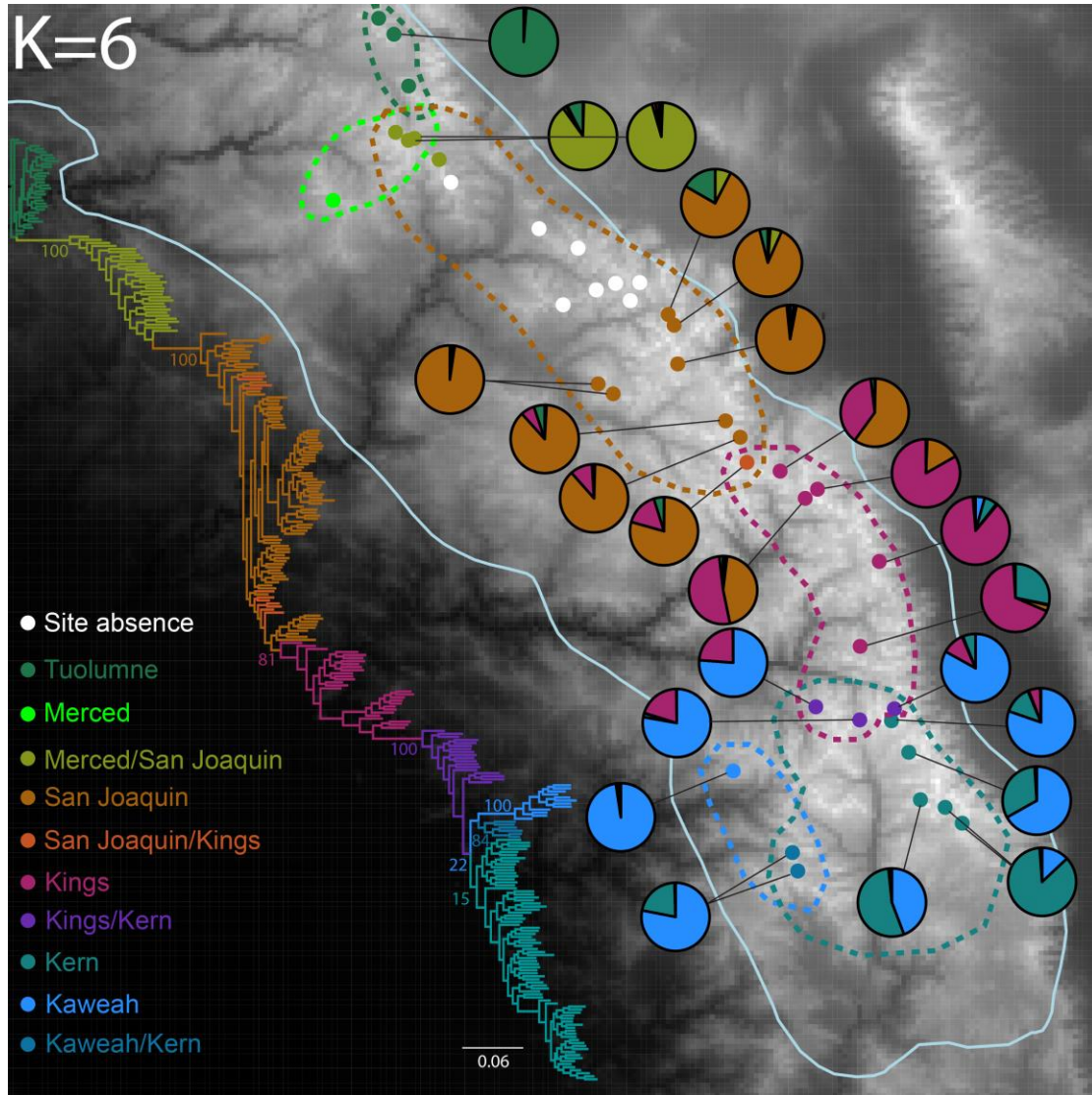


21

22 **Figure 3.** The SNAPP species tree of individuals from eight sites using the
 23 *fully-filtered* SNP dataset. The thick black line shows the consensus tree, and the
 24 numbers at each node denote the posterior probability.

25

26

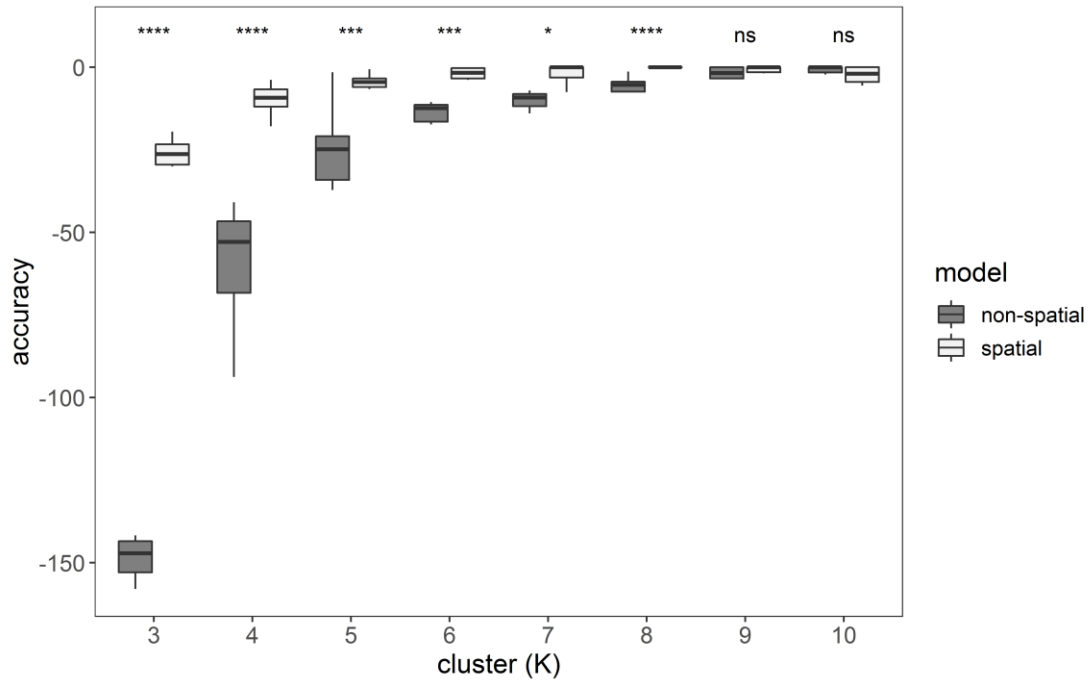


27

28 **Figure 4.** Population structure of the *N. ingens* complex based on sNMF clustering
 29 analysis for K=6 (left) and K=10 (right). The concatenated ML tree is shown on the
 30 K=6 map with bootstrap support for major nodes. The colors of population clusters
 31 and clades reflect the major drainage basins of the Sierra Nevada, and the drainage is
 32 roughly circled by the dashed lines.

33

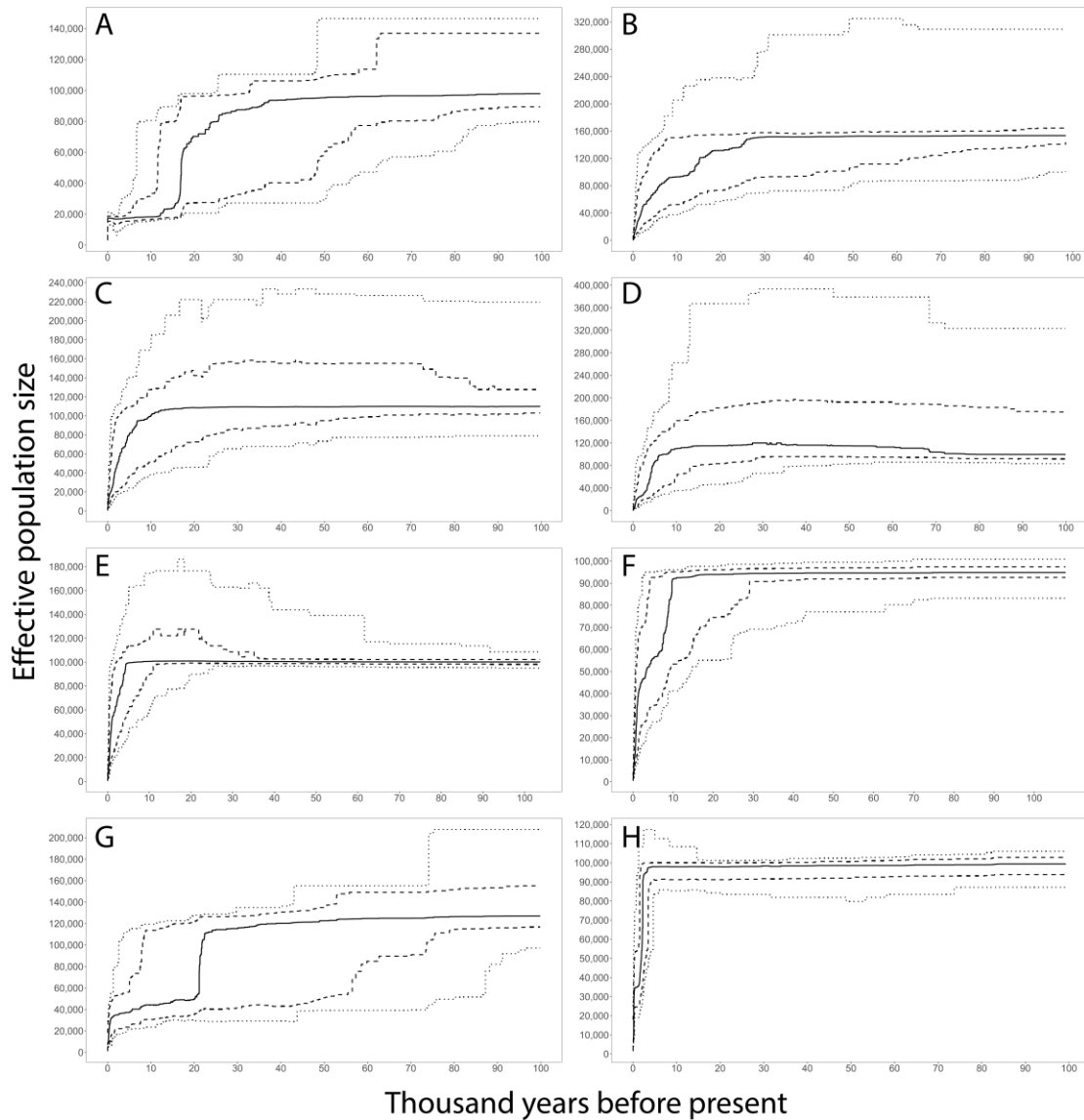
34



35

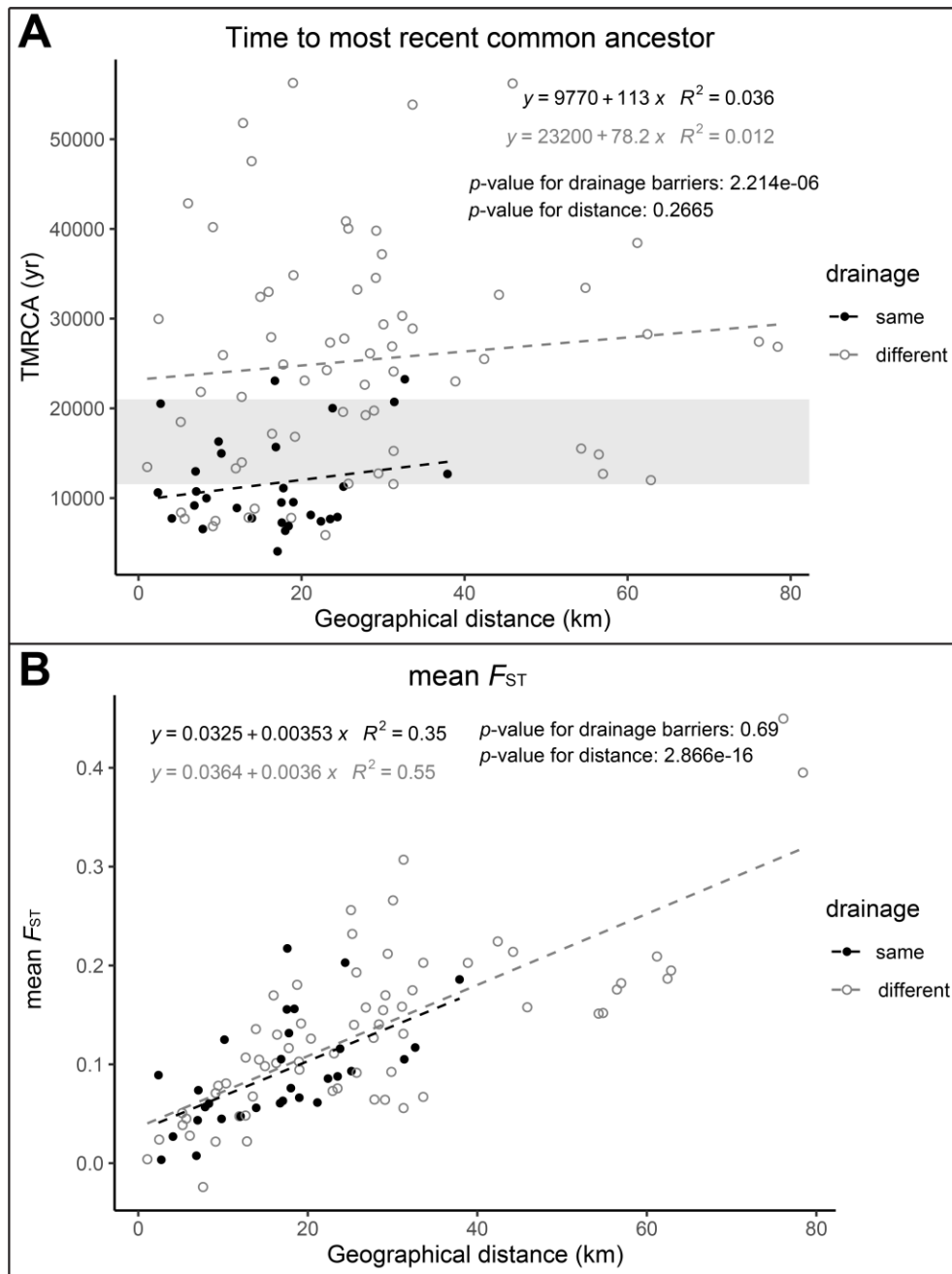
36 **Figure 5.** The model accuracies estimated using conSturct. For the K=3 to K=8,
 37 spatial models are significantly more accurate than non-spatial models ($p < 0.05$).
 38

39



40
41
42
43
44
45
46
47

Figure 6. Stairway plots of eight selected sites including site 1 (A), site 3 (B), site 9 (C), site 10 (D), site 12 (E), site 17 (F), site 26 (G), and site 27 (H). The solid lines, dashed lines, and dotted lines represent the median, 12.5% and 87.5%, and 2.5% and 97.5% confidence intervals, respectively. All sites show dramatic population declines in past 30 thousand years.



48

49 **Figure 7.** Measurements of TMRCA (A) and F_{ST} (B) for paired populations from the
 50 same (solid circle) and different (empty circle) drainages, plotted against geographical
 51 distance. For TMRCA (A), there is a significant difference between same and
 52 different drainage population pairs, with no significant correlation between TMRCA
 53 and geographical distance. The TMRCA across different drainages mostly predates
 54 the last glacial maximum (LGM), which is denoted by the grey box. For F_{ST} (B), there
 55 is no significant difference between population pairs within and among drainages, but
 56 the correlation between F_{ST} and geographic distance is significant